Electronic Supplementary Material (ESI) for Nanoscale.

Supplementary

Electromechanical conversion efficiency of GaN NWs: Critical influence of the NW stiffness, the Schottky nano-contact and the surface charge effects

Noelle Gogneau[1], Pascal Chrétien[2], Tanbir Sodhi[1,2], Laurent Couraud[1], Laetitia Leroy[1], Laurent Travers[1], J.C. Harmand[1], François H. Julien[1], Maria Tchernycheva[1], Frédéric Houzé[2]

[1] *Centre de Nanosciences et Nanotechnologies, Université Paris-Saclay, CNRS, UMR9001, Boulevard Thomas Gobert, 91120 Palaiseau, France*
[2] *Université Paris-Saclay, CentraleSupélec, Sorbonne Université, CNRS, Laboratoire de Génie électrique et électronique de Paris, 11 rue Joliot-Curie, 91190 Gif sur Yvette, France*

S1: "*Classical*" AFM characterization technique using standard contact mode to quantify the piezoelectric response of vertically oriented-NWs laterally bent by the AFM tip during scanning.

The quantification of the energy conversion of NW arrays by conductive AFM tip measurements have been first performed under the "classical" configuration, in which the AFM tip scans over the array of vertically oriented-NWs in the standard contact mode [1-2]. The NWs are subjected to an external lateral force resulting from the mixture of the controlled constant normal force (CNF) and the lateral force resulting from the tip/sample relative displacement. The AFM tip induces a lateral bending of the nanostructures. In response to this deflection and due to the piezoelectric effect, the NW generates an output voltage, which is simultaneously measured through the conductive AFM tip. This experimental characterization procedure is performed without any external polarization of the nanostructures. It is based on an Ohmic contact formed between the NWs and the substrate, and on a Schottky contact formed at the interface between the NWs and the conductive AFM tip [3,4].

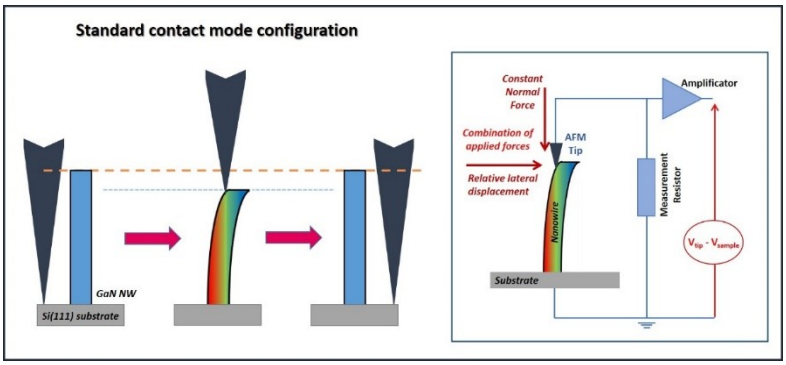

Fig. S1: Schematic representations of an AFM equipped with an electrical module used in contact mode to perform piezoelectric generation measurement on laterally bent NWs.

S2: Establishment of piezoelectric potential in *laterally bent* NWs.

Under lateral deformation, the NWs are characterized by the appearance of an asymmetric strain evolving from a negative to a positive value respectively at the compressed and stretched sides of the nanostructures. In response to this deformation, an asymmetric piezoelectric field is created inside the NWs with a sign depending on the NW polarity. Depending on the distribution of potential within the bent NW, on the doping of the NW and on the position of the conductive tip on its surface, the Schottky junction can be reverse-biased or forward-biased [1, 5].

In the present paper, we are studying nitrogen (N^{2-}) polar GaN NWs presenting a p-type doping. As a consequence, the piezoelectric potential is evolving from negative at the stretched NW side to positive at the compressed NW side, and the Schottky diode is forward biased when the tip is in contact with the compressed side, thus allowing to harvest the piezo-generated energy [6].

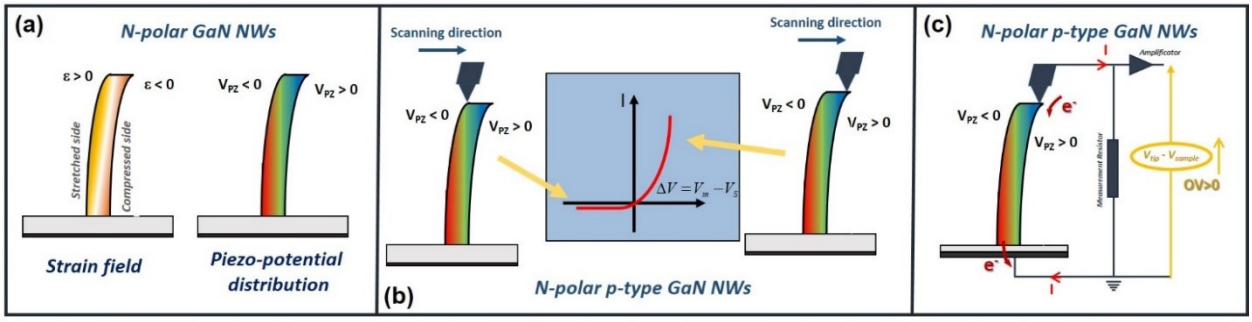

Fig. S2: (a) Schematic representations of the strain field and piezo-potential distribution inside an N-polar GaN NW laterally bent by a conductive AFM tip. (b) Schottky contact established between the top of the NW and the conductive AFM tip. In presence of N-polar p-type doped GaN NWs, the Schottky diode is forward biased when the diode is in contact with the positive piezoelectric potential created inside the NW. (c) Equivalent electrical circuit for N-polar p-type doped GaN NWs.

S3: Establishment of piezoelectric potential in *axially compressed* N-polar p-doped GaN NWs.

Under axial compression, the N-polar p-type GaN NWs are characterized by the appearance of a negative strain. In response to this deformation, a positive piezo-potential is created within the top portion of the NW [6]. The GaN NWs being p-doped, the Schottky diode deposited directly on the top portion is forward biased and thus allows the energy harvesting by the AFM tip.

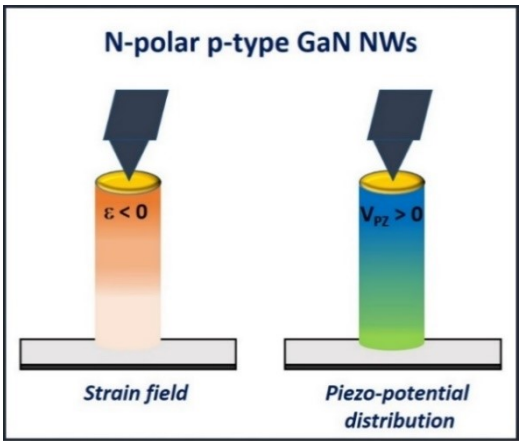

Fig. S3: Schematic representations of the strain field and piezo-potential distribution inside an N-polar p-type doped GaN NW axially compressed by a conductive AFM tip

S4: Quantification of the NW stiffness.

<u>Hooke's law:</u>

The stiffness has been quantified by using the equation:

$$F = k.\Delta l$$

where F is the axial constant normal force (CNF), Δl is the NW height variation measured from topographic images in response to its compression under the action of F (Fig. S4.1a), and k is the stiffness, corresponding to the slope of the linear fitting of the $F=f(\Delta l)$ curve as illustrated on Fig. S4.1b.

The determination of Δl implies the knowledge of the initial length, l_0, of the measured NW. Unfortunately, once the AFM tip is in contact with the NW, this one is axially compressed, even for weak applied forces. The extracted length, l, is thus different from the initial one. To evaluate l_0, we have plotted the evolution of the measured height as a function of the CNF as illustrated in Fig. S4.1c. By linearly fitting the curve, l_0 can be calculated from the y-intercept.

Remark: As explained in the manuscript, due to the mechanical consolidation of the NWs with the soft matrix to ensure reliable measurements, the NW height measured by AFM corresponds to the height of the emerging portion of the NW (denoted $H_{consol\text{-}NW}$ in Fig.2.b). The height of the soft matrix has been added to provide the complete dimensions of the nanostructures.

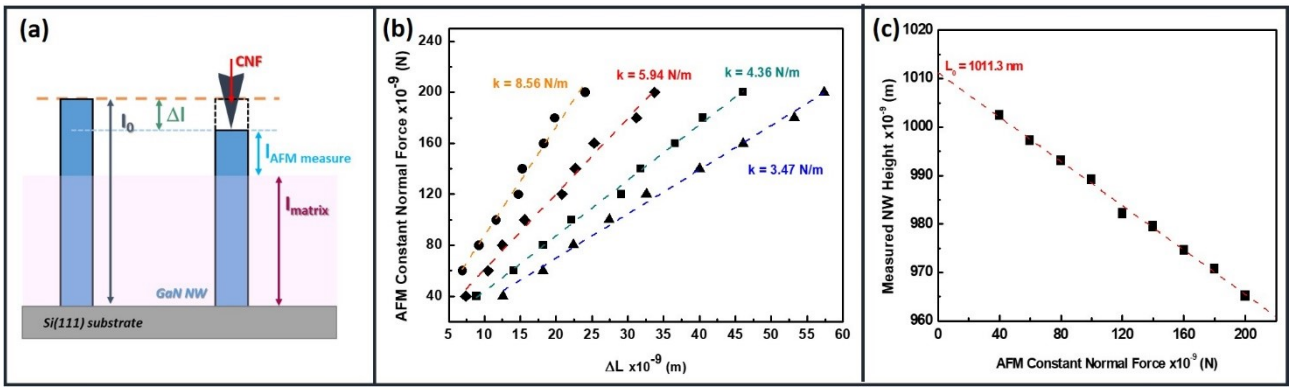

Fig. S4.1: (a) Schematics of the NW showing their various dimensions; (b) Variation of the NW height, Δl, measured from topographic AFM images as a function of the axial constant normal force applied by the AFM tip, for four different NWs. The slope of the fitted curves (dashed lines) corresponds to the NW stiffness; (c) Variation of the NW height as a function of the CNF.

The *F=f(Δl)* plot shows a linear dependence for low to moderate applied forces (≤ 200 nN) as shown on Fig. S4.2. This behavior indicates an increase of the NW compression with the CNF. At higher *F* and for the NWs of lower stiffness, the data deviate from the ideal Hooke law, Δ*l* being larger than expected. This indicates that these NWs start to bend under the action of the CNF.

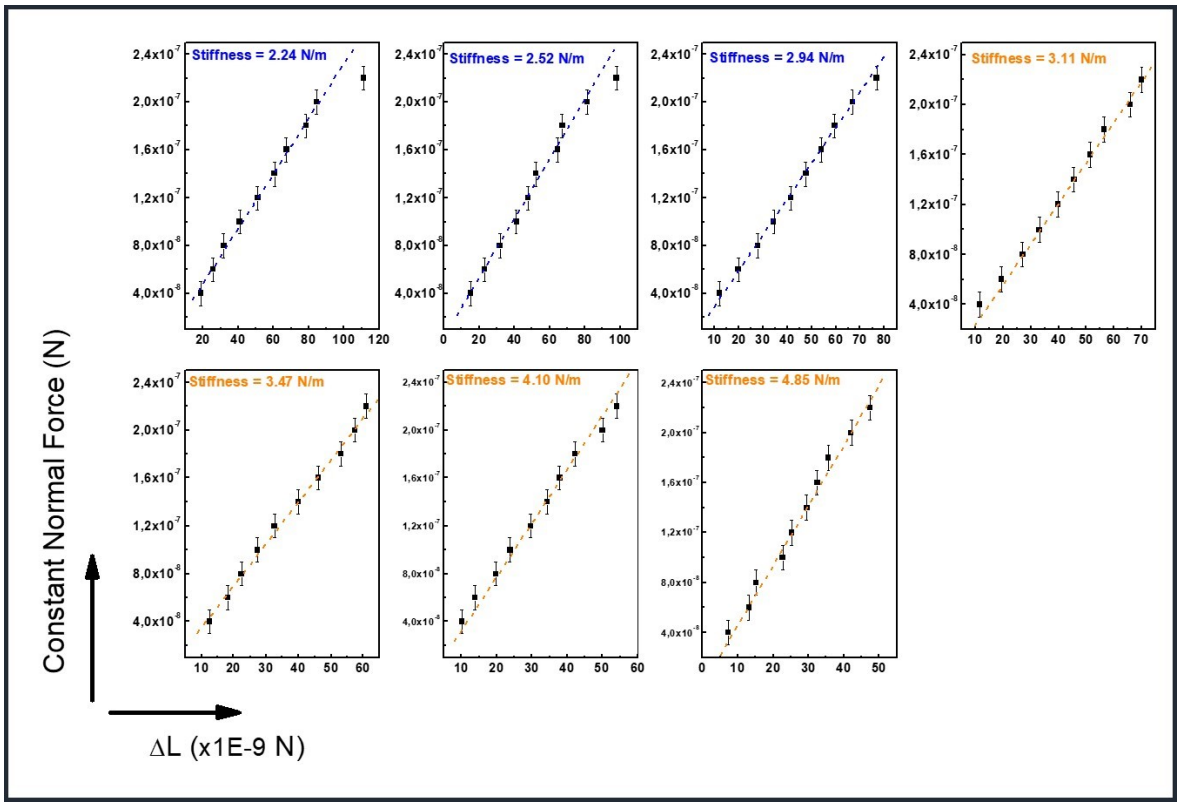

Fig. S4.2: Variation of the NW height, Δl, measured from topographic AFM images as a function of the axial constant normal force applied by the AFM tip, for stiffness evolving between 2 and 5 N/m. For stiffness between 3 and 5 N/m, the compression of the NW is quasi linear indicating an increase of the NW compression with the CNF. By contrast, for stiffness lower than 3 N/m, the Δl deviates from the linear behavior, indicating that the NW in addition to be compressed, also presents a bending under the action of CNF. This Δl deviation increases as the stiffness is decreasing.

Elasticity theory:

The stiffness has also been quantified through considering the elastic modulus δ given by:

$$\sigma = \delta.\varepsilon$$

where σ and ε are respectively the stress and the strain within the NW induced by the application of the external force, and k' is the stiffness, corresponding to the slope of the linear fitting of the $\sigma=f(\varepsilon)$ curve.
σ and ε have been quantified by using NW characteristics measured from topographic images and the following equations:

$$\sigma = F/\pi R^2$$

where F is the normal force applied axially and R is the NW radius measured by taking into account the AFM tip/surface convolution

$$\varepsilon = \Delta l/l_0$$

where Δl is the NW height variation measured as explained in the Hooke law part and l_0 is the initial height of the NWs.

The $\sigma = f(\varepsilon)$ plot shows an equivalent dependence with the CNFs.

S5: Electromechanical coupling coefficient.

The electromechanical coupling coefficient is given by:

$$\eta = \frac{output\ electrical\ energy}{input\ mechanical\ energy} = \frac{\Delta W_{PZT}}{\Delta W_{ELD}} \qquad (1)$$

I- The input mechanical energy

The input mechanical energy corresponds to the elastic deformation energy for compressing/releasing the NW.

The deformation of the NW under an axial force is expressed through the formula defining the Young's modulus E:

$$E = \frac{Stress}{Strain} = \frac{F/A_0}{\Delta l/l_0}$$

or using the (x, y, z) coordinates:

$$E = \frac{F/A_0}{Z_m/Z_0} \qquad (2)$$

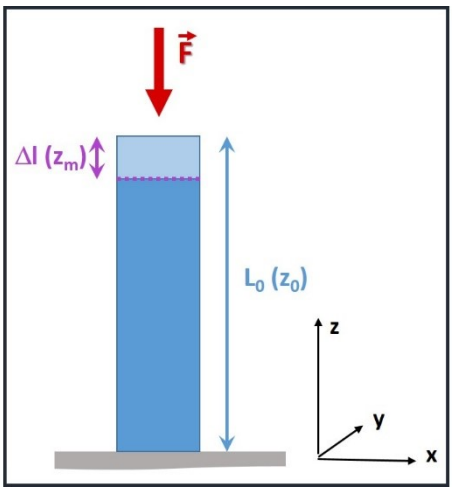

Fig. S5: Schematic representation of the NW

where F is the applied CNF, A_0 is the NW section supposed unchanged, l_0 is the initial NW height, and Δl is the NW height variation measured from topographic images in response to its compression under the action of F.

For each cycle, during the compression phase, the applied force f, increasing from 0 to F, may be expressed as

$$f = \frac{E\,A_0\,Z}{Z_0} \qquad (3)$$

The mechanical work done by this external force for axially compressing the NW is given by:

$$W_{ELD} = \int_{f=0}^{f=F} f dl = \int_{0}^{Z_m} f(Z) dZ$$

$$W_{ELD} = \frac{EA_0}{Z_0} \int_{0}^{Z_m} Z \, dZ$$

$$W_{ELD} = \frac{1}{2} \frac{EA_0}{Z_0} Z_m^2 \quad (4)$$

After one cycle of pure axial mechanical input, including, along the z-axis, the mechanical compression of the NW under the AFM tip applied force, and the mechanical decompression of the NW at the AFM tip releasing, we assume that the elastic energy loss is given by:

$$\Delta W_{ELD} = 2 * W_{ELD} = \frac{EA_0}{Z_0} Z_m^2 = \frac{EA_0}{l_0} \Delta l^2 = F \Delta l \quad \textbf{(5)}$$

II- Output piezoelectric energy

The capacitance associated to the charges generated by an individual NW in one piezoelectric discharge is given by

$$C = \frac{\tau}{R_{total}} = \frac{\tau}{R_L + R_S + R_{NW}} \quad (6)$$

where τ is the decay time of the system and R_{total} is the resistance of the system corresponding to the sum of the load resistance R_L, the series resistance R_S of the Schottky diode through which is harvested the OV and the NW resistance R_{NW}.

According to the discharge of an RC circuit [1], the output electric energy generated by an individual NW in one piezoelectric discharge is given by:

$$\Delta W_{PZT} = \frac{1}{2} C V^2 \quad (7)$$

With equation (6), and by considering that with our measurement method, the R_S value includes the NW resistance, R_{NW}, this gives:

$$\Delta W_{PZT} = \frac{1}{2} \frac{\tau}{2R_L + R_S} V^2 \quad \textbf{(8)}$$

where V is the piezo-generated OV and R_L $(1\ G\Omega)$ is the load resistance. R_S (144 MΩ) has been evaluated from I(V) characteristics performed on various single NWs. By fitting the curve dV⁄dLnI=f(I) to a straight line and by using the following equation, $\frac{dV}{dLnI} = n\frac{k_B T}{q} + IR_S$, R_S can be determined from the slope of the line. Finally τ $(3\ ms)$ is the decay time of the system, integrating both the τ_{cirt} of the electronic circuit and the τ_{NW} of the NW.

Table S1: Average values, standard deviations and maximum output voltages (measured with a precision of 2%) piezo-generated by GaN NWs under well-controlled axial Constant Normal Force.

Constant Normal Force (nN)	Average Output Voltage/Standard Deviation (mV) *Double Distribution of the Output Voltages*		Maximum Output Voltage (mv)
	Distribution 1	***Distribution 2***	
40	*8,7 ± 7,5*	*31,4 ± 10,5*	*79*
60	*12,5 ± 10,7*	*40,8 ± 12,8*	*92*
80	*15,4 ± 13,2*	*44,7 ± 11,1*	*104*
100	*16,5 ± 15,0*	*54,4 ± 10,2*	*111*
120	*17,8 ± 13,8*	*55,0 ± 15,8*	*118*

140	*19,3 ± 12,1*	*61,1 ± 18,2*	*130*
160	*22,2 ± 13,1*	*69,0 ± 20,4*	*138*
180	*26,0 ± 19,3*	*79,9 ± 17,6*	*156*
200	*29,1 ± 20,4*	*88,7 ± 21,3*	*159*
220	*31,9 ± 25,3*	*78,1 ± 24,4*	*153*

Supplementary references

[1] Wang, Z.L., Song, J. Piezoelectric nanogenerators based on zinc oxide nanowire arrays. *Science* **2006**, *312*, 242–246.

[2] Gogneau, N., Chrétien, P., Galopin, E., Guilet, S., Travers, L., Harmand, J-C., Houzé, F. GaN nanowires for piezoelectric generators. *Phys. Status Solidi RRL* **2014**, *8*, 414–419.

[3] Jacopin, G., De Luna Bugallo, A., Rigutti, L., Lavenus, P., Julien, F. H., Lin, Y-T., Tu, L-W., Tchernycheva, M. Interplay of the photovoltaic and photoconductive operation modes in visible-blind photodetectors based on axial p-i-n junction GaN nanowires. *Appl. Phys. Lett.* **2014**, *104*, 023116.

[4] Liu, J., Fei, P., Song, J., Wang, X., Lao, C., Tummala, R., Wang, Z. L. Carrier Density and Schottky Barrier on the Performance of DC Nanogenerator. *Nano Lett.* **2008**, *8*, 328–332.

[5] Gogneau, N., Jamond, N., Chrétien, P., Houzé, F., Lefeuvre, E., Tchernycheva, M. From single III-nitride nanowires to piezoelectric generators: New route for powering nomad electronics. *Semicond. Sci. Technol.* **2016***, 31*, 103002.

[6] Gogneau, N., Chrétien, P., Galopin, E., Guilet, S., Travers, L., Harmand, J-C., Houzé, F. Impact of the GaN nanowire polarity on energy harvesting. *Appl. Phys. Lett.* **2014**, *104*, 213105.